

# Molecular-Beam Mass-Spectrometry to Ammonium Dinitramide Combustion Chemistry Studies

Oleg P. Korobeinichev,\* Leonid V. Kuibida,† Alexander A. Paletsky,‡ and Andrey G. Shmakov§  
*Russian Academy of Sciences, 630090 Novosibirsk, Russia*

The methods for the study of flame structure and kinetics of the thermal decomposition of solid propellant by probing mass spectrometry are described. The developed methods were applied to the study of ammonium dinitramide (ADN) combustion chemistry. The study has shown that along with ADN decomposition, sublimation takes place to give gaseous ADN followed by dissociation to yielding ammonia and dinitramine acid (HD). Gaseous ADN has been observed in ADN decomposition products. The structure of ADN combustion zones at 1–6 atm was studied using a molecular-beam mass-spectrometry as well as a microthermocouple technique. Three combustion zones have been observed. Gaseous ADN has been discovered in the first cool flame zone at 3 atm. Gaseous ADN dissociation on  $\text{NH}_3$  and HD followed by HD decomposition in the near-surface zone are key reactions resulting in a temperature rise of about 150 K. The second high-temperature zone is found within 6–8 mm from the ADN burning surface at 6 atm. The main reaction in this zone is ammonia oxidation by nitric acid and the combustion temperature is 1400 K. The third zone was observed at 40 atm, the measured final temperature was ~2000 K. The obtained data form the basis for the development of a chemical mechanism of reactions in both the ADN flame and combustion model.

## Introduction

It is generally believed that future progress in solid propellant (SP) combustion studies will result in a better understanding of the chemistry and physics taking place in SP flames. It is important to understand combustion chemistry because it is the type of information a propellant formulator or chemist may use to tailor and/or improve the performance of the propellant.<sup>1</sup> The main sources of our knowledge on the combustion chemistry of SP are the results of flame structure studies: Spatial distributions of temperature and species concentration in flame.<sup>2–4</sup> The main methods applied to the investigation of chemical and thermal flame structures of SP are 1) probing mass-spectrometry (MS)<sup>2–6</sup>; 2) spectroscopic methods—absorption and emission,<sup>1,7,8</sup> planar laser-induced fluorescence (PLIF),<sup>8</sup> spontaneous Raman scattering (SRS), and coherent anti-Stokes Raman Spectroscopy (CARS)<sup>9</sup>; and 3) a microthermocouple technique.<sup>10</sup> Until recently, there were few works on SP flame structure. However, with an improvement in experimental technique, the development of works on flame structure modeling, and the rise of interest in SP combustion chemistry, the number of works in this field has increased.

At the present time, one of the most effective and universal experimental techniques for studying SP flame structure is the method of mass-spectrometric probing of SP flames (MSPSPF).<sup>11</sup> This method allows the detection of all species present in the flame as well as the determination of their concentrations and spatial distributions, i.e., the study of flame microstructure. The method of probing MS is also successfully

applied for the study of the kinetics and mechanisms of SP thermal decomposition. Thermal decomposition of SP is one of the most important stages of the SP combustion process. The reactions taking place in the surface layer of burning SP are suppliers of gas products whose subsequent reactions result in heat release sustaining the combustion process. Kinetics and reaction mechanisms of SP thermal decomposition and their ingredients at a temperature close to that at the burning surface are necessary to understand the combustion mechanism and development of an SP combustion model. Such information can result from the use of rapid-scan Fourier transform infrared (FTIR) spectroscopy, simultaneous mass and temperature change- (SMATCH-) FTIR, or T-Jump/FTIR, developed by Brill et al.,<sup>12</sup> as well as the method of differential mass-spectrometric thermal analysis (DMTA) discussed in Ref. 13. It allows the acquisition of information about the products of SP decomposition as well as the rate of evolving each product as a function of time.

The purpose of this work is to describe an MS probing technique and to demonstrate examples of its application to the study of ammonium dinitramide (ADN) flame structure, thermal decomposition, and combustion chemistry. ADN is a new energetic material that can be used as an oxidizer in solid rocket propellants.<sup>14</sup> It presents an alternative to ammonium perchlorate (AP), being an ecologically pure oxidizer in solid propellants. The possibility of a detailed study of its combustion mechanism on a molecular level and the development of a model of its combustion seems likely because of its chemical structure simplicity, and relatively small number of possible products.

The results of experimental studies of ADN thermal decomposition and combustion are found in the literature.<sup>5,6,12,15–27</sup> A manometric method was applied to ADN thermal decomposition at a low temperature (up to 170°C) in liquid and solid.<sup>16</sup> Another paper deals with the thermal decomposition of ADN thin films applied to a platinum filament at 1 atm.<sup>12</sup> The filament was heated with electricity to 260°C (the heating rate is ~2000°C/s), which was maintained to be constant. Decomposition products were recorded with an FTIR-spectrometer. ADN decomposition under  $\text{CO}_2$ -laser support (heat flow 20–200 W/cm<sup>2</sup>) at a pressure from 0.1 to 3 atm in Ar was studied.<sup>6</sup> The decomposition product ratio was analyzed using probing

Received Sept. 20, 1997; presented as Paper 98-0445 at the AIAA 36th Aerospace Sciences Meeting, Reno, NV, Jan. 12–15, 1998; revision received April 3, 1998; accepted for publication April 5, 1998. Copyright © 1998 by the American Institute of Aeronautics and Astronautics, Inc. All rights reserved.

\*Professor, Head of Laboratory, Institute of Chemical Kinetics and Combustion Siberian Branch. E-mail: korobein@ns.kinetics.nsc.ru.

†Ph.D., Senior Researcher, Institute of Chemical Kinetics and Combustion Siberian Branch.

‡Researcher, Institute of Chemical Kinetics and Combustion Siberian Branch.

§Postgraduate Student, Institute of Chemical Kinetics and Combustion Siberian Branch.

MS. The initial results of an ADN thermal decomposition under nonisothermic conditions obtained using MS thermal analysis are represented.<sup>18,19</sup> A product, which has been assigned by mass-spectra as  $\text{NH}_2\text{NO}_2$  (62 amu), was found in the products of ADN flameless combustion at 1 atm (self-sustaining thermal decomposition) together with products that were observed earlier ( $\text{NH}_3$ ,  $\text{HNO}_3$ ,  $\text{NO}_2$ ,  $\text{N}_2\text{O}$ ,  $\text{NO}$ , and  $\text{N}_2$ ).<sup>18</sup> The mechanism of ADN decomposition has been studied theoretically<sup>15</sup> and experimentally<sup>20</sup> at 140–170°C by FTIR-spectroscopy and MS. Nitramide has been detected, but dinitraminic acid has not been found. The thermal decomposition of ADN has been studied by differential scanning calorimetry (DSC) and thermal gravimetry combined with mass-spectrometry (TG-MS). The product gases have been identified by MS as  $\text{NH}_3$ ,  $\text{H}_2\text{O}$ ,  $\text{NO}$ ,  $\text{N}_2\text{O}$ ,  $\text{NO}_2$ ,  $\text{HONO}$ , and  $\text{HNO}_3$ .<sup>21</sup> Temperature-controlled gas cell and thin-film laser-pyrolysis techniques have been used to investigate the condensed-phase thermal decomposition of ADN at temperatures between 60 and 400°C. Thermal decomposition products have been monitored by FTIR spectroscopy.<sup>22</sup> Both experimental techniques show that the primary decomposition products are  $\text{N}_2\text{O}$  and  $\text{NO}_2$ . Thermal decomposition of ADN and  $^{15}\text{N}$  and  $^{21}\text{N}$  isotopomers have been studied in Ref. 23. In gas-cell experiments Russell et al.<sup>24</sup> detected the formation of  $\text{N}_2\text{O}$  at a low temperature (60°C). The structures, energies at 0 K, and enthalpies at 298 K have been computed for 37 molecules, ions, and transition states that have been implicated in the thermal decomposition of ADN.<sup>25</sup> These data permit the calculation of  $\Delta H$  (298 K) for a large number of possible decomposition steps; some of these results are presented and discussed. The thermal decomposition behavior of ADN has been investigated using different thermoanalytical techniques.<sup>26</sup> The main decomposition products are  $\text{NH}_4\text{NO}_3$ ,  $\text{N}_2\text{O}$ , and  $\text{H}_2\text{O}$ . Additional gaseous decomposition products are  $\text{NO}_2$ ,  $\text{NO}$ ,  $\text{NH}_3$ ,  $\text{N}_2$ , and  $\text{O}_2$ , detected by FTIR and MS. Extensive measurements have been made of ADN diffusion flames.<sup>27</sup> ADN was found to have diffusion flames with energetic binders at low pressures, but they were very far from the surface. The combustion of sandwiches based on ADN and a binder was studied in an effort to understand the combustion mechanism of ADN-based composite systems. Temperature profiles in ADN combustion waves have been measured using thin thermocouples.

### Experimental Techniques

The probing MS method consists of the following: A burning strand of SP moves with a speed exceeding the burning rate toward a probe, so that a probe is continuously sampling gaseous species from all of the zones, including those adjacent to the burning surface. The sample is transported to an ion source of a time-of-flight (TOF) or quadrupole MS. Mass spectra of samples are recorded with simultaneous filming of the probe and the burning surface.

Two types of apparatuses have been developed to study flame structure. The sample is transported to an ion source as a molecular flow using a microprobe with the inlet orifice of 10–20  $\mu\text{m}$  in the first type of setup and as a molecular beam using a sonic probe with the inlet orifice of 20–200  $\mu\text{m}$  in the second type. The former setup has a high spatial resolution and just slightly disturbs the flame, allowing study of the flame with a narrow combustion zone up to 0.1 mm. However, in this case, radicals recombine and unstable species can decompose and react on the inner walls of the probe. The latter setup with molecular beam mass-spectrometric (MBMS) sampling allows the detection of radicals and other unstable species, but more strongly disturbs the flame and, therefore, has a reduced spatial resolution.

The MBMS system (Fig. 1) has been used to examine ADN flame structures.<sup>2–4</sup> It includes an apparatus for probing a flame containing a molecular beam-sampling system, a time-of-flight mass-spectrometer (TOFMS)-type MSKh-4 as a detector, a combustion chamber, a scanning system, a data acquisition

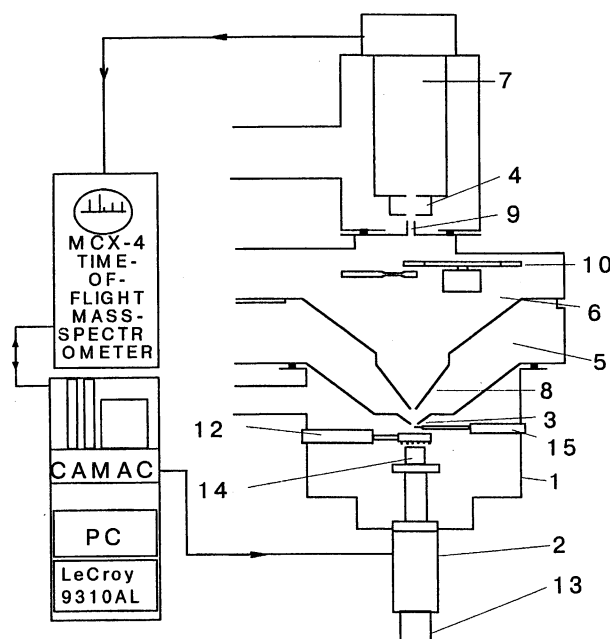


Fig. 1 MBMS system for studying the flame structure of solid propellants with TOFMS. 1, combustion chamber; 2, scanning system; 3, probe; 4, ion source; 5, skimmer chamber; 6, collimator; 10, slotted disk; 11, electromagnetic chopper; 12, ignition spiral; 13, stepper motor; 14, burning strand; and 15, thermocouple.

system, and an experiment controller based on computer assistance for measurements and control (CAMAC) equipment and a computer.

The flame is sampled with a probe (3), a 25-mm-high cone with a 50-deg-external angle, a 40-deg-internal angle, and a 50–100- $\mu\text{m}$ -diam orifice at the apex (at 1 atm). A probe produces a molecular beam, which passes to an ion source. The ignition spiral (12) is automatically removed from the combustion zone after ignition. To scan the SP flame a control system and a stepper motor (13) are required. The burning strand (14) is moved with a motor (13). Thermocouple (15) serves to measure the temperature profile in flames. A strand is moved at a speed less than 20 mm/s and is driven by a stepper motor, step – 2.5  $\mu\text{m}$ . The data acquisition and control system consists of an AT486 computer, a CAMAC apparatus, a double-beam oscilloscope, a scanner control, and a printer. To study the flame structure at high pressures with an MBMS quartz probe with an inner angle of 40 deg and with an orifice of 50  $\mu\text{m}$  at 3 atm, 20  $\mu\text{m}$  at 6 atm and a wall thickness near the probe tip of 25  $\mu\text{m}$  was used. For visualization of the combustion process a Panasonic NV-M3000EN video cameras was used. The study of an  $\text{H}_2/\text{O}_2/\text{Ar}$  (0.1/0.05/0.85) flame structure stabilized on a flat burner at 10 atm was carried out to demonstrate the possibility of an MBMS application for the study of flame structures at high pressures.<sup>28</sup>

CAMAC equipment measured a number of chosen mass peak intensities as functions of time. However, it is not always possible to predict which peaks are to be found in a mass-spectrum. To reveal peaks in a mass-spectrum, a LeCroy-9310AL oscilloscope with a memory of 1 Mbyte was used. It allowed the detection of singular mass spectra within short time intervals, e.g., ~0.01 s (frequency of oscilloscope start is 2 KHz, 50 accumulations), which was impossible using available CAMAC equipment. At a starting frequency (frequency of the singular mass-spectra record) of 400 Hz a mode of information cyclic record in memory was used that provided oscilloscope operation within –1.5 s. To stop data from being recorded into the oscilloscope memory when the probe came in contact with the burning surface, a special device was designed and constructed. An end switch of the step motor device moving the sample to the probe was used as a sensor, keeping

a record of contact. Video recording from the ADN strand-burning surface and probe was performed concurrently with the mass-spectra recording. This two-measurement synchronization was achieved by allowing the contacts of the step motor device end switch to close at the moment of probe contact with the strand-burning surface. The latter was accompanied by light diode luminescence concurrently with the stoppage of a step-frequency generator, which stopped the LeCroy oscilloscope. Light diode luminescence was recorded with a video camera. The developed scheme allowed experimental determination of the burning surface location on mass peak intensity profiles.

In some cases temperature profiles were measured by an immovable thermocouple, in other cases a thermocouple was moved toward a strand's burning surface with a scanning device at a rate exceeding the burning rate. Pt–PtRh (10%) and WRe (20%)–WRe (5%) thermocouples with 20–30- $\mu\text{m}$ -diam wire were used. The time constant for the Pt–PtRh (10%) thermocouple with a diameter of 20  $\mu\text{m}$  and a length of 3 mm was found to be 0.004 s. The temperature in ADN combustion products at 6 atm was measured with a thermocouple Pt–PtRh (10%),  $\sim 120$   $\mu\text{m}$  total diameter. The width of thermocouple wires was 50  $\mu\text{m}$ . The thermocouple was protected with a Ceramobond 569 anticatalytic coating. The coating width was 35  $\mu\text{m}$ . The thermocouple arm length was 2 mm. The time constant in this case was 0.05 s. Thermocouple outlets were placed in quartz capillaries 5 mm in length and 0.5 mm in diameter and fastened to the ceramic tube. The thermocouple was inserted between igniter loops made from nichrome wire. The thermocouple junction was situated within  $\sim 1$ –2 mm below the plane where igniter loops were located. The distance between the thermocouple and ADN strand surface was  $\sim 0.2$ –0.5 mm.

MS investigations of SP's thermal decomposition kinetics, which are similar to those present in the condensed phase of the SP's burning surface and method, are detailed in Ref. 2. ADN thermal decomposition was studied at  $10^{-6}$  torr, 6 torr, 100 torr, and 1 atm within 100–300°C. The ADN sample was placed in a tantalum (in the experiments at 100 torr and 1 atm) or tungsten (at  $10^{-6}$  torr) ribbon, whose temperature was measured with a chromel–copel thermocouple [the copel is 43% Ni, 0.5% Mn, and 55.5% Cu (by mass)] fastened on by pressure contact welding. A similar procedure was first developed for the study of AP decomposition.<sup>29</sup>

For the study of ADN thermal decomposition in vacuum at  $10^{-6}$  torr, a sample was deposited to the surface of tungsten ribbon from an aqueous solution. The mass of the applied sample ranged from  $10^{-4}$  to  $10^{-5}$  g, it was about 0.5  $\mu\text{m}$  thick. The tungsten ribbon was 0.1 mm thick, 1 mm wide, and 2 cm long. A chromel–copel thermocouple 50  $\mu\text{m}$  in diameter was welded onto the ribbon. The substance was applied at the side opposite to the site of thermocouple welding. Ribbons were heated either by discharge from a charged capacitor (heating time 0.01 s) or by passing electric current from a power source, providing a constant temperature to the ribbon.

Decomposition products were recorded with a TOFMS. For the experiments in vacuum ( $10^{-6}$  torr) the ribbon with a substance was placed in an ion source chamber under its inlet or on its side (Fig. 2). In the first case the interaction of the primary reaction products with the walls falls far short of expectations.

To study ADN decomposition in a flow reactor at 100 torr and 1 atm, molecular-beam probing MS was employed (Fig. 3). A tantalum ribbon 2.5 mm wide, 0.1 mm thick, and  $\sim 3$  cm long was placed in a 1-cm-diam quartz tube. The ribbon was curved inside the tube. A chromel–copel thermocouple 50  $\mu\text{m}$  in diameter was welded onto the ribbon by pressure contact welding.

Argon flow was supplied through the tube (about 15  $\text{cm}^3/\text{s}$ ). ADN decomposition products were conveyed with argon flow to the probe of the MBMS inlet system. The distance from the

ribbon with the ADN sample to the probe orifice was about 2 mm. The mass of ADN sample was  $10^{-4}$  g. Particular emphasis should be placed on the fact that mass peak intensities vary directly with the rate of corresponding products evolving an ADN decomposition in both variants of the experiment (Figs. 2 and 3). The sole exception is provided by the case of very high decomposition rates in vacuum when the pumping rate of each product should be considered. Methods of data processing for both cases are described.<sup>30,31</sup>

A quartz flow reactor was used to study ADN decomposition at 6 torr and 80–140°C. Argon flow of about 50  $\text{cm}^3/\text{min}$  normal temperature and pressure (NTP) passed through the 0.25-g ADN sample and distributed a thin layer on the surface of the reactor. Residence time was about  $10^{-2}$  s. To provide a more profound study of ADN sublimation at 6 torr a so-called "two-temperature flow reactor" was used. It represented two quartz reactors heated to different temperatures and connected in series with each other (Fig. 4). ADN samples weighing 0.25–0.45 g ( $m_1$ ) distributed in a thin layer along the reactor

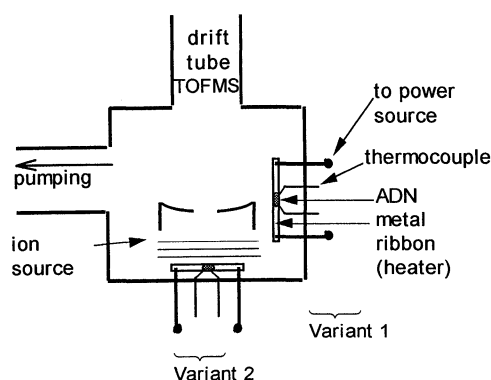


Fig. 2 Setup for ADN thermal decomposition at pressure  $10^{-7}$ – $10^{-5}$  torr.

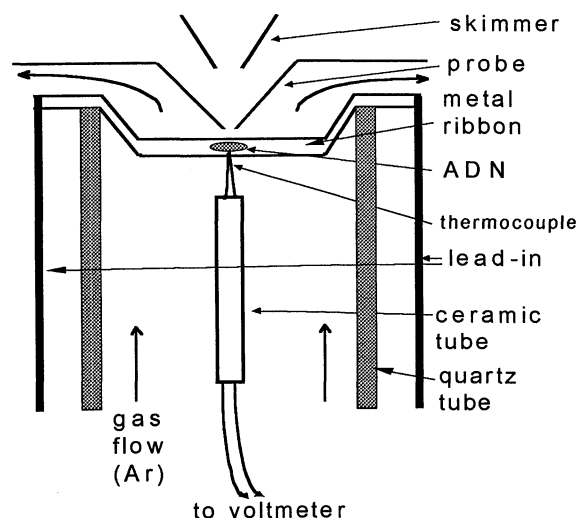


Fig. 3 Flow reactor for ADN thermal decomposition at pressure 100 torr and 1 atm.

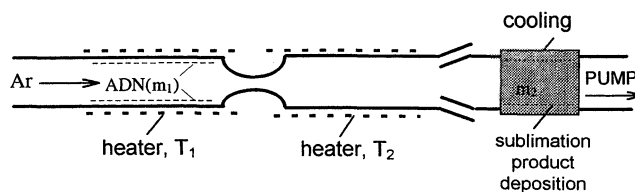


Fig. 4 Installation with a two-temperature flow reactor ( $T_1$ ,  $T_2$ ) for the study of ADN decomposition and kinetics of the reactions of ADN decomposition at 6 torr.

surface were placed in the first reactor heated to 140°C. The second reactor was heated to  $t_2 \geq t_1$ . Sublimation products were deposited on unheated tube parts as the ADN samples left reactor 2.

The dry mass of the deposited products  $m_2$  was defined as  $m_1$  by weighing. In another case the flow reactor was combined with another MBMS setup that had been used earlier for the study of an  $H_2/O_2/Ar$  low-pressure flame (Fig. 5) doped with organophosphorous compounds.<sup>32</sup> In this case the probe orifice was about 0.5 mm and a modulated component of the molecular beam was detected by a quadrupole MS.

To obtain quantitative characteristics of decomposition or combustion product compositions, the mass-spectra of individual species  $H_2O$ ,  $NO$ ,  $N_2O$ ,  $NO_2$ ,  $HNO_3$ ,  $N_2$ , and  $NH_3$  were obtained and their calibration coefficients  $k_i$  were measured:  $k_i = I_{Ar}P_i/I_iP_{Ar}$ , where  $I_{Ar}$  and  $I_i$  are the intensities of argon or  $i$ -species peaks, respectively; and  $P_{Ar}$  and  $P_i$  are the corresponding partial pressures in the combustion chamber or in the reactor. The mole fraction in our experiment was defined as

$$\alpha_i = I_i k_i / (\sum I_j k_j) \quad (1)$$

where  $I_i = I_{i(\text{exp})} - \sum I_{j(i)}$ ;  $I_i$  = mass peak intensity of  $i$  species;  $I_{i(\text{exp})}$  = initial experimental intensity; and  $\sum I_{j(i)}$  = the intensities sum of inputs  $j$  species into  $I_{i(\text{exp})}$ .

ADN used in this work were synthesized at the Zelinsky Institute of Organic Chemistry Russian Academy of Sciences by the method described in Ref. 33. The purity of ADN is 97%. The main impurity is ammonium nitrate (AN) (less than 3%). Melting starts at 90–94°C. Decomposition starts at 130–135°C. The specific density of ADN crystal is 1.82 g/cm<sup>3</sup>. ADN strands are 21 mm in length, 10 mm in diameter, and a specific density of 1.79 g/cm<sup>3</sup> pressed using 7000 atm.

## Results

Decomposition at 1 atm: A sample of ADN (crystals,  $\sim 10^{-4}$  g) was placed in a flow reactor under nonisothermal conditions, and the temperature of thermal decomposition starting at 1 atm was determined at constant heating with a rate of about 90°C/s. A "step" compatible with the melting point of about 90°C and endothermic process is found on the curve of temperature dependence on time. The following mass peaks were found in decomposition product mass-spectra (the ions responsible for them are cited in parentheses): 17 ( $NH_3^+$ ,  $OH^+$ ), 18 ( $H_2O^+$ ), 28 ( $N_2^+$ ), 30 ( $NO^+$ ), 44 ( $N_2O^+$ ), and 46 ( $NO_2^+$ ). At about 215°C the formation of ADN decomposition products is

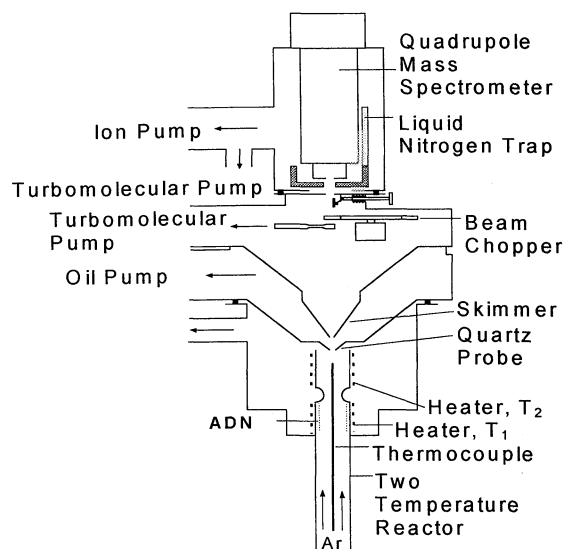


Fig. 5 Mass-spectrometric setup with a two-temperature flow reactor for the study of ADN decomposition and kinetics of the reactions of ADN at 6 torr.

found to start (Fig. 6). Concurrently, the ribbon temperature jumps to  $\sim 290^\circ\text{C}$ , which bears witness to an exothermic process. The rise of mass peaks 18 and 44 are first found in the mass-spectrum, and then the other peaks are found to rise. Table 1 shows mass peak intensities at two sites corresponding to 1) the maximal intensity of peak 18 and 2) the maximal intensity of peaks 46, 30, and 17.

Decomposition at 100 torr: This decomposition was also performed in a flow reactor with molecular-beam sampling in argon flow (Fig. 7). The heating rate was about 90°C/s. No fluctuations common to the experiments at 1 atm are found on the temperature curve. Mass peaks intensities are shown in Table 2 at their maximum.

Decomposition at 6 torr: The sublimation process in the total decomposition process increases under low pressures. ADN decomposition at 80–140°C in a flow reactor (in the flow of

Table 1 Relative mass peak intensities<sup>a</sup>

<i>m/e</i>	$I_i/I_{17}$	$T^\circ\text{C}$
17	1	215
	1	290
18	4.3	215
	1.16	290
28	0.3	215
	0.17	290
30	1.7	215
	1.27	290
44	1.3	215
	0.22	290
46	1.5	215
	1.72	290

<sup>a</sup> In mass-spectra of ADN decomposition products at 1 atm.

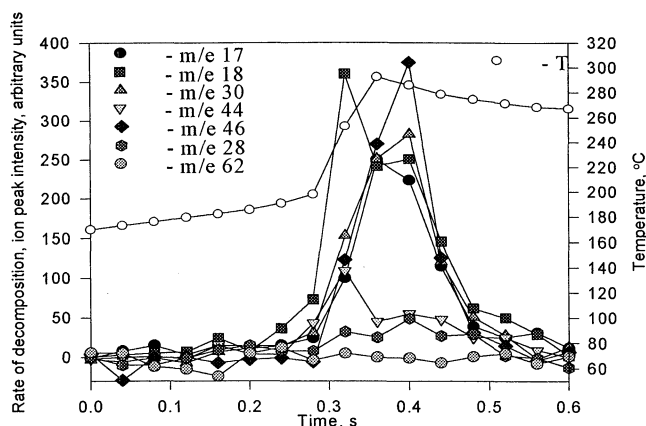


Fig. 6 Thermal decomposition of ADN at 1 atm.

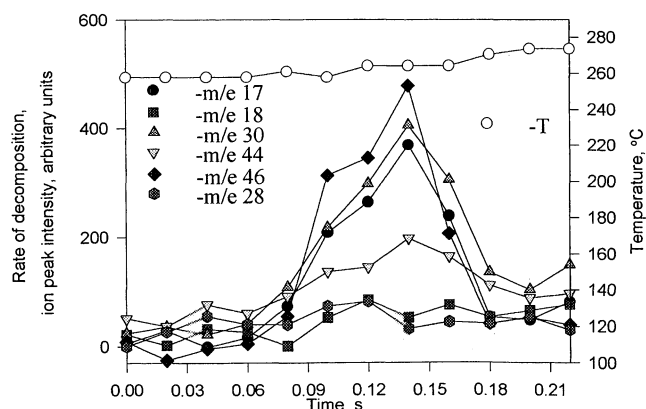


Fig. 7 Thermal decomposition of ADN at 100 torr.

**Table 2** Relative mass peak intensities<sup>a</sup>

<i>m/e</i>	<i>I<sub>i</sub>/I<sub>17</sub></i>	<i>T</i> °C
17	1	270
18	0.12	270
28	0.04	270
30	1.08	270
44	0.4	270
46	1.4	270

<sup>a</sup>In mass-spectra of ADN decomposition products at 100 torr.

**Table 3** Fraction of ADN deposit (*m<sub>2</sub>/m<sub>1</sub>*) and mass peak ratios at exit of reactor 2 as a function of reactor 2 temperature

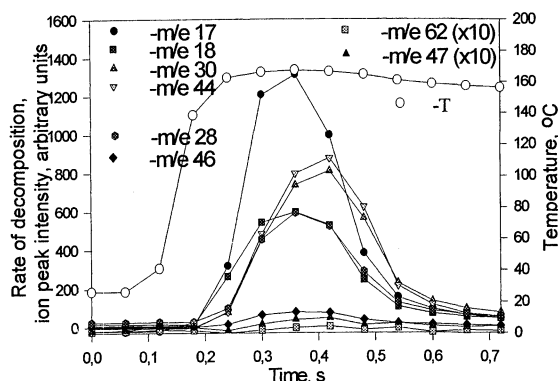
<i>T<sub>2</sub></i> , °C	<i>m<sub>2</sub>/m<sub>1</sub></i>	<i>I<sub>46</sub>/I<sub>20</sub></i>	<i>I<sub>30</sub>/I<sub>20</sub></i>	<i>I<sub>17</sub><sup>*</sup>/I<sub>20</sub></i>
160	0.93	0.20 ± 0.01	0.12 ± 0.01	0.07 ± 0.01
240	0.70	0.16 ± 0.01	0.25 ± 0.02	0.12 ± 0.01
320	0.17	0.10 ± 0.01	0.30 ± 0.03	0.13 ± 0.02
450	0	0.10 ± 0.01	0.31 ± 0.01	0.10 ± 0.01

argon) at 6 torr showed that >90% of ADN was deposited on the cold wall of the tube of the flow reactor's exit. The absence of mass peak 63 in the mass-spectra and, consequently, the absence of nitric acid in ADN decomposition products should be noted. The most intensive peak is the one of mass 46. Also mass peaks 18 (H<sub>2</sub>O), 17 (H<sub>2</sub>O, NH<sub>3</sub>), 16 (NH<sub>3</sub>), and a weak mass peak 44 (N<sub>2</sub>O) were found. The ratio of mass peaks 30 and 46 (*I<sub>30</sub>/I<sub>46</sub>* is about 0.5) is such that mass peak 46 cannot be assigned to NO<sub>2</sub> (the ratio *I<sub>30</sub>/I<sub>46</sub>* is 6.2 in NO<sub>2</sub> mass-spectrum). In these experiments at a low pressure initial sublimation stage needs to be found: ADN vapors generation or dissociation into ammonia and acid (dinitraminic acid), similar to that for other ammonium salts, e.g., ammonium nitrate. Sublimation product identifications and their mass-spectra recording allow the qualitative and quantitative interpretation of combustion products mass-spectra in the most important flame area, the nearby ADN burning surface. It is noteworthy that according to the theoretic predictions<sup>15</sup> on the ab initio calculation basis, the mechanism for ADN decomposition in the early stage is dominated by the following reaction:



hereafter HN(NO<sub>2</sub>)<sub>2</sub> and [NH<sub>3</sub>] · [HN(NO<sub>2</sub>)<sub>2</sub>] will be called HD and ADN<sub>l</sub>, respectively. The energy of ADN evaporation yielding ADN<sub>l</sub>, according to the calculations,<sup>15</sup> is as much as 38 kcal/mole, whereas the energy of ADN<sub>l</sub> dissociation yielding NH<sub>3</sub> and HD is 12–14 kcal/mole, and the energy of ADN<sub>l</sub> dissociation yielding NH<sub>3</sub> and HD is 50–52 kcal/mole. We do not know of any experimental evidences supporting these theoretical predictions. In these experiments *m<sub>2</sub>* (the mass of deposited ADN) at the reactor temperature of *T<sub>1</sub>* = 140°C was shown to fall with the reactor temperature *T<sub>2</sub>* rise from 160 to 320°C as represented in Table 3.

In Table 3 *I<sub>17</sub><sup>\*</sup>* = the intensity of mass peak 17 minus the input from mass peak 18 (H<sub>2</sub>O<sup>+</sup>) and *I<sub>20</sub>* = the intensity of mass peak 20 (Ar<sup>+</sup>). MS analysis of products leaving the second reactor (Table 3) have shown that mass peak 46 decreases 2.0 times, and mass peaks 30 and 17 rise ~2.6 and ~1.4 times correspondingly, and that the ratio of *I<sub>46</sub>/I<sub>30</sub>* changes from 1.67 to 0.32 with a temperature increase from 160 to 320°C. Similar experiments on ADN decomposition–sublimation at 6 torr and 140°C were carried out on the setup shown in Fig. 1. The following ratios for the peaks in ADN decomposition (sublimation) products mass-spectrum were found: *I<sub>30</sub>/I<sub>46</sub>* = 0.5, *I<sub>17</sub>/I<sub>46</sub>* = 0.35; and *I<sub>44</sub>/I<sub>46</sub>* = 0.1, which are close to those cited in Table 3. We believe that the obtained

**Fig. 8** Thermal decomposition of ADN at low pressure (10<sup>-7</sup>–10<sup>-5</sup> torr).

data support theoretical predictions found in Ref. 15. The formation of complex ADN<sub>l</sub> is the first stage of ADN decomposition. Decomposition product mass-spectra at 160°C correspond to ADN<sub>l</sub>. In the second reactor (160–320°C) ADN<sub>l</sub> decomposition takes place to give NH<sub>3</sub> and HD. Decomposition product mass-spectra at 320–450°C correspond to mass-spectra NH<sub>3</sub> and HD sum. The NH<sub>3</sub> + HD reaction with formation deposition ADN<sub>l</sub> does not occur at the exit from reactor 2 heated to 450°C, because the ADN<sub>l</sub> formation from NH<sub>3</sub> and HD does not take place because the reaction is exothermic (12–14 kcal/mole), but occurs (similar to radicals recombination) as a result of a trimolecular reaction (with participation of the third body). At 6 torr these reactions proceed at a very low rate. This conclusion is supported by our tests on AN thermal decomposition under the same conditions. AN decomposition products heating to 400°C in reactor 2 do not effect the AN deposition as it leaves reactor 2 (in this case *m<sub>2</sub>/m<sub>1</sub>*), because in this case the process occurs in one stage heterogeneously (not in volume). Additional support to the preceding conclusion is the temperature dependence *p*<sup>\*</sup> of ADN sublimation vapors we have found. It was defined by weighing ADN deposits at the flow reactor 1 exit (there was no reactor 2 in this case) at its different temperatures (within the range of 80–140°C) and ADN decomposition time. This dependency is expressed by the formula

$$\lg p^* = 19.58 - 8.77 \times 10^3/T$$

where *p* = pressure (torr) and *T* = temperature (K). Sublimation heat corresponding to this dependency is Δ*H<sub>subl</sub>* ≈ 40 kcal/mole, which is close to the calculation results at the first stage,<sup>15</sup> 38 kcal/mole. Should ADN<sub>l</sub> decomposition yielding HD and NH<sub>3</sub> be the first stage of the process, the temperature dependence of HD + NH<sub>3</sub> vapors would correspond to the half-value of this process heat, i.e., 25–26 kcal/mole. An effective rate constant of ADN vapor decompositions found as a result of processing the experiments on ADN vapor decompositions in the second reactor also agrees with the suggested assumption

$$k_{ef} = 10^6 \times \exp(-E/RT), \text{ s}^{-1}$$

where the reaction activation energy *E* = 11.5 kcal/mole is close to the value of the reaction endothermal barrier (~12 kcal/mole).

Decomposition in high vacuum (10<sup>-5</sup>–10<sup>-7</sup> torr): Results of experiments are shown in Fig. 8 and Table 4.

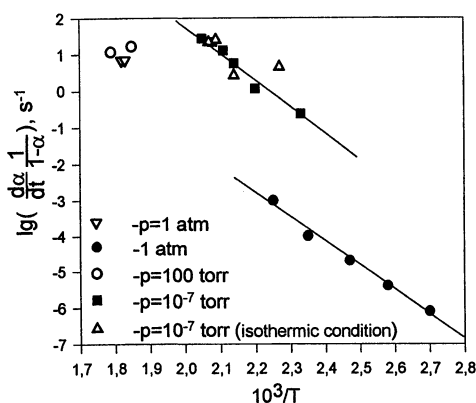
Using the dependence of the ADN decomposition rate on the fraction of decomposition at low pressure under isothermic conditions, the first-order reaction of decomposition has been determined. An Arrhenius plot of ADN rate is presented in Fig. 9. The reaction rate constant in vacuum has been found:

$$W = \frac{d\alpha}{dt} = 3.5 \times 10^{15} \left[ \exp \left( \frac{-32,000}{RT} \right) \right] (1 - \alpha), \text{ s}^{-1}$$

**Table 4** Relative mass peak intensities<sup>a</sup>

<i>m/e</i>	<i>I<sub>i</sub>/I<sub>17</sub></i>	<i>T</i> °C
17	1	167
18	0.5	167
28	0.5	167
30	0.84	167
44	0.8	167
46	0.08	167

<sup>a</sup>In mass-spectra of ADN decomposition products in high vacuum.

**Fig. 9** Arrhenius plot for ADN decomposition rate constant.

The analysis of the data obtained showed mass-spectra of ADN decomposition products at 1 atm, 6 torr, and 100 torr to differ significantly from the mass-spectra of ADN decomposition products in vacuum, especially the ratio  $I_{46}/I_{17}$ , which comprises 1.5–1.7 in the first case, whereas in vacuum  $I_{46}/I_{17} = 0.06$ –0.16.  $\text{ADN}_v$  is then adsorbed by the vacuum chamber walls when decomposed in vacuum and was not found in a mass-spectrum, whereas  $\text{ASN}_v$  was found in a flow reactor case. At a high pressure (1 atm and more), the ADN decomposition rate under the conditions close to those of combustion can be controlled with the  $\text{ADN}_v$  decomposition rate (as it is controlled in the case of AP decomposition under the combustion conditions with  $\text{HClO}_4$  decomposition).

### ADN Flame Structure

ADN strands burn steadily and flamelessly at 1 and 3 atm. The flame appears at the ADN deflagration at 6 atm. Different methods were applied to measure the burning rate: Those based on signals from thermocouples and mass-spectra of a strand ignition and extinction (at 1, 3, and 6 atm) and on video-recording data (at 6 atm). The results of studying the burning rate and final burning temperature at different pressures (1–40 atm) are tabulated in Table 5.

Comparing ADN burning rate data for 3 and 6 atm with those obtained in Ref. 17 for twice-recrystallized ADN shows satisfactory agreements between them. Therefore, the impurity of AN in ADN has no noticeable effect on the ADN burning rate. Two types of experiments on MS probing of the ADN burning zone have been conducted:

1) A strand mounted 1 mm from the probe is immovable, thus the burning surface is moving outward from the probe at the ADN burning rate.

2) the burning strand is moving toward the probe at a rate exceeding the ADN burning rate. Both methods were used when determining combustion product compositions at 1 and 3 atm. The following masses have been experimentally detected in the mass spectra of samples withdrawn from combustion products: 46 ( $\text{NO}_2$ ,  $\text{HNO}_3$ ,  $\text{ADN}_v$ , HD); 30 ( $\text{NO}$ ,  $\text{N}_2\text{O}$ ,  $\text{NO}_2$ ,  $\text{HNO}_3$ ,  $\text{ADN}_v$ , HD); 44 ( $\text{N}_2\text{O}$ ); 17 ( $\text{NH}_3$ ,  $\text{H}_2\text{O}$ ,  $\text{ADN}_v$ ); 28 ( $\text{N}_2$ ,  $\text{N}_2\text{O}$ ); 18 ( $\text{H}_2\text{O}$ ); and 63 ( $\text{HNO}_3$ ).

**Table 5** Burning rate  $\mu$  and final temperature of ADN combustion products  $T_c$  in relation to pressure *p*

<i>p</i> , atm	$\mu$ , mm/s	<i>T<sub>c</sub></i> , °C
1	$3.44 \pm 0.05$	$345 \pm 25$
3	$11 \pm 1$	$540 \pm 80$
6	$19 \pm 2$	$1080 \pm 30$
40	$55 \pm 5$	1700

Results of ADN combustion products at 1 atm: The relative peak intensities  $I_i/I_{44}$  in the mass-spectra are  $m/e = 17, 18, 28, 30, 44, 46, 62$ , and 63; and  $I_i/I_{44} = 0.78, 0.35, 0.26, 1.4, 1, 1.3, 6.3 \times 10^{-3}$ , and  $1.1 \times 10^{-3}$ .

Along with the previously mentioned mass peaks a peak of 62 amu was found, whose intensity exceeded the 63-amu peak by a factor of 5–6. The peak of 62 amu has not yet been identified. It may be assigned to nitramide  $\text{NH}_2\text{NO}_2$  or possibly the  $\text{NO}_3$  radical. Identification requires calibration by these specific compounds. The nature of peaks' behavior with time (seldom sharp fluctuations) is indicative of the formation of AN aerosol, most likely from the  $\text{NH}_3$  and  $\text{HNO}_3$  reactions in the gas phase.

To identify ADN combustion products at  $p = 1$  atm by their mass-spectra, the experiments were performed where the condensed combustion products were frozen in a trap cooled with frozen ethanol ( $-113^\circ\text{C}$ ), and noncondensed products ( $\text{N}_2$  and  $\text{NO}$ ) were pooled in a special vessel. When defreezing the trap, AN (in the dry deposit) as well as  $\text{H}_2\text{O}$  and  $\text{N}_2\text{O}$  were found. MS analysis of noncondensed gasses has shown that they involve nearly only  $\text{N}_2$  (with  $\text{NO}$  traces). Quantitative products analyses gave the following composition of combustion products. The mole fractions  $\alpha_i$  of ADN combustion products at 1 atm based on direct measurements: Species =  $\text{H}_2\text{O}$ ,  $\text{N}_2\text{O}$ ,  $\text{NH}_3$ ,  $\text{HNO}_3$ , and  $\text{N}_2$ ; and  $\alpha_i = 0.35, 0.4, 0.1, 0.1$ , and 0.05. (0.1 were obtained using the dry deposit.)

We did not succeed in finding ADN in combustion products by direct methods, possibly because of its small amounts and inadequate accuracy in analyzing dry deposits. From the preceding products compositions we have found corresponding mass-spectrum. Subtraction of this mass-spectrum from the experimentally obtained one has shown that the unidentified remaining mass-spectrum involves mass peaks 17, 30, and 46. Peaks ratios in the remaining mass-spectrum corresponds to these peak ratios in the mass-spectrum of  $\text{ADN}_v$ . A contradiction was found between the results of the ADN burning surface temperature measurements and the calculations using an equation of enthalpy conservation and product compositions near an ADN burning surface. The contradiction disappears when sensitivity coefficients by  $\text{ADN}_v$  that are higher than the experimentally measured ones are taken. It is assumed that the reason for such divergence is found at the difference conditions of the temperature and pressure in calibrations by  $\text{ADN}_v$  (6 torr) and combustion (1–3 atm). The  $\text{ADN}_v$  cluster formation is likely to occur on sampling under the combustion conditions. Thorough analysis gave the following composition for ADN combustion products at 1 atm. Species =  $\text{H}_2\text{O}$ ,  $\text{N}_2\text{O}$ ,  $\text{NH}_3$ ,  $\text{HNO}_3$ ,  $\text{N}_2$ , and  $\text{ADN}_v$ ; and  $\alpha_i = 0.33, 0.38, 0.11, 0.09, 0.05$ , and 0.03.

Results of ADN flame structure study at 3 atm: A visual observation of ADN burning at 3 atm has shown that a luminous flame is not likely to be observed under these conditions. Figure 10 represents mass peak intensity and temperature profiles in the zone adjacent to the ADN burning surface at 3 atm. Reference to Fig. 10 shows that all peaks decrease to a variable extent. The greatest decrease is observed for peaks 46, 30, and 17. Initially the decrease of all peaks seems strange. However, an account must be taken of the fact that both initial compounds (which are consumed), and final products (which are accumulated), bear input into the peaks; besides having dif-

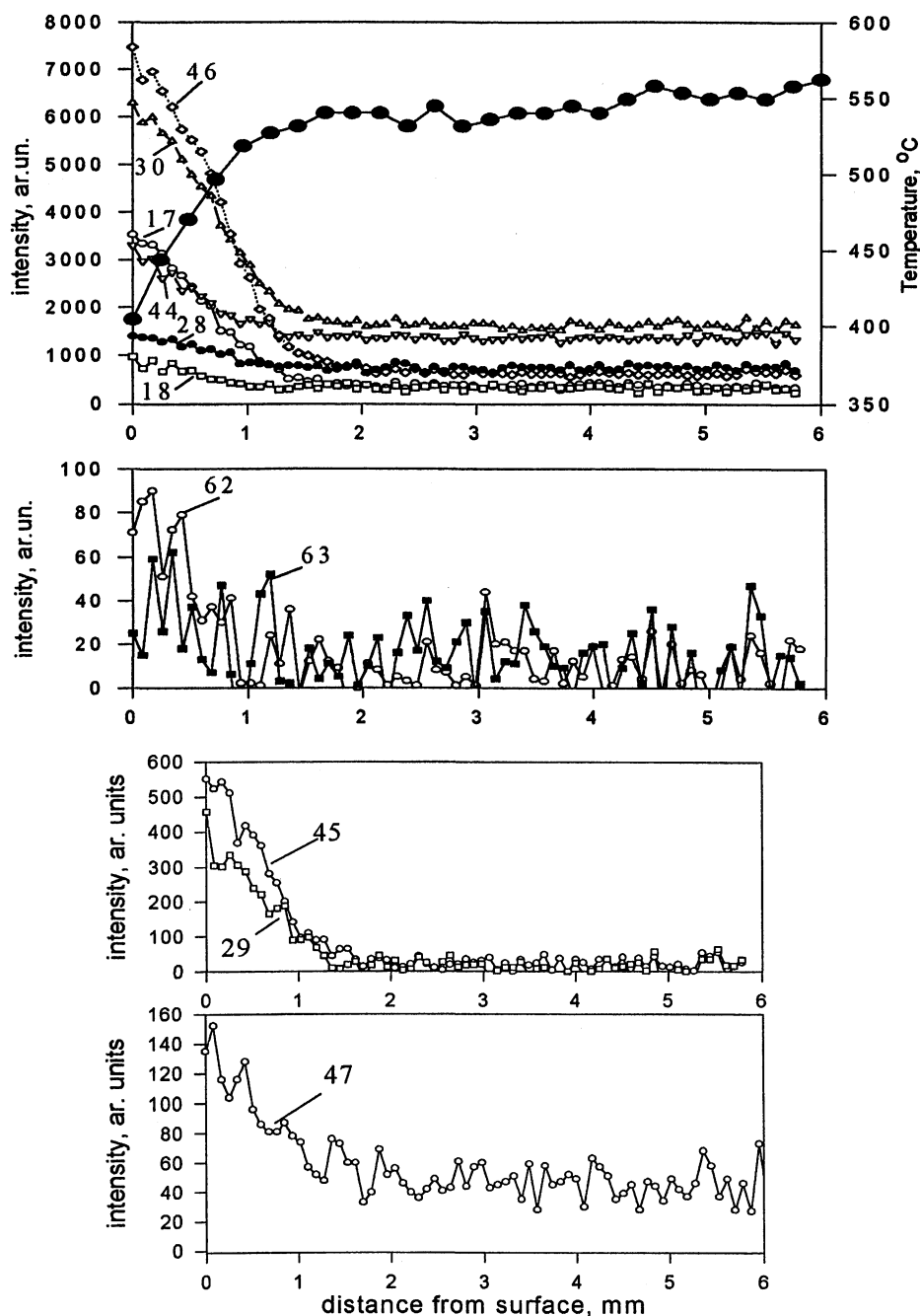


Fig. 10 Mass-peak intensities of ADN flame  $p = 3$  atm.

ferent calibration coefficients. The analysis of Eq. (1) for the calculation of species concentrations using peak intensities in mass-spectra and calibration coefficients shows that in the given case the initial species concentration falls, and the combustion product grows.

Mass-spectra areas 17–69 and 100–110 amu were recorded in the experiments when the burning strand is moving toward the probe at a rate exceeding the ADN burning rate (on probing the zone adjacent to the burning surface) using the LeCroy 9310AL oscilloscope with a memory of 1 MB. We have succeeded in recording a near-surface zone at the relative rate of the burning-strand movement toward the probe equal to 17.5 mm/s (the ADN burning rate was 10 mm/s). In these experiments concurrent mass-spectra and temperature recording was performed using an uncoated thermocouple that was 50  $\mu\text{m}$  in diameter. The latter was situated 1 mm from the probe inlet orifice in the plane perpendicular to its axis. These experiments allowed new (as compared with the previously mentioned

ones) mass peaks of 29, 45, 47, and 62. A narrow zone of cool (invisible) flame  $\sim 1.5$  mm was found near the burning surface, where a change (decrease) in absolute intensities of mass peaks 29, 45, 47, 62, and 63 as well as 46, 30, 17, 44, 28, and 18 takes place. This is accompanied by a temperature rise from 400 to 550°C in this zone (Fig. 10).

Mass peaks 29 and 45 are assumed to be fragmentary ions from either nitramide  $\text{NH}_2\text{NO}_2$  ( $\text{N}_2\text{H}^+$  29 amu,  $\text{HN}_2\text{O}^+$  45 amu) or ADN, and its decomposition products (or fragmentary ions from all of these compounds). Peak 47 amu that can be interpreted as HONO was found in the combustion products. The rise of peak 47 amu intensity near the combustion surface can be associated with possible input from ADN, into peak 47 amu. The intensity of peak 47 amu in the combustion products cannot be associated with  $^{15}\text{N}$  isotope excess. The isotope ratio is  $^{15}\text{N}/^{14}\text{N} = 0.0037$  and  $I_{47}/I_{46}$  is 0.05 in the combustion products.

The assumption about the presence of  $\text{NO}_2$  and  $\text{HNO}_3$  cannot provide an explanation to the high intensity of peak 46



**Table 6** Product composition (in mole fractions) in ADN cool flame at 3 atm at different distances from the burning surface

L, mm	NH <sub>3</sub>	H <sub>2</sub> O	N <sub>2</sub>	NO	N <sub>2</sub> O	ADN <sub>v</sub>	HNO <sub>3</sub>	HONO	NO <sub>2</sub>	Element balance N:H:O
0.2	0.08	0.30	0.08	0.19	0.24	0.03	0.08	—	—	1.11:1.04:1.09
3	0.07	0.31	0.08	0.16	0.25	0	0.08	0.03 <sup>a</sup>	0.03 <sup>a</sup>	1.03:0.94:1.05

<sup>a</sup>Included based on analysis.

(Fig. 10) in the near zone of the ADN combustion products at 3 atm. The ratio of the remaining mass peaks 46 and 30 is  $\sim 1.3$  with regard to the input from 46 (NO<sub>2</sub>) and 63 (HNO<sub>3</sub>) into peak 30, and the input from 63 (HNO<sub>3</sub>) into peak 46. If the remainder from peak 30 is believed to be associated only with NO<sub>2</sub> (NO is absent), the input from NO<sub>2</sub> into peak 46 would account for 10% from the experimentally measured one. The consideration of NO will give less input from NO<sub>2</sub> into peak 46. That is why the main part of peak 46 is not attributable to the presence of NO<sub>2</sub> and the input from HNO<sub>3</sub>. We have suggested that the input from NO<sub>2</sub> into peak 46 to a first approximation can be ignored. Based on the results of the research in the ADN decomposition–sublimation at 6 torr, we suggest that peak 46 be assigned to ADN, with the peak ratios  $I_{17}:I_{30}:I_{44}:I_{46} = 0.35:0.5:0.1:1$  measured on the same setup where the ADN flame structure was studied. The ratio of peaks 63 and 46 in the final combustion products corresponds to the HNO<sub>3</sub> mass-spectrum. However, because of the error in the intensity measurements of mass 63 of low value, the neglected NO<sub>2</sub> mole fraction can possibly be as much as 0.03. When defining the combustion products compositions, NH<sub>2</sub>NO<sub>2</sub> is not considered because of peak  $m/e$  62 low intensity ( $I_{62}/I_{46} \sim 0.005$ ), an inadequately large input from it into peak 46 amu, and the absence of calibrations because of the lack of the product. This input ( $I_{46} = 5 \times I_{62}$ ) was evaluated based on the results of an analysis where an attempt to obtain NH<sub>2</sub>NO<sub>2</sub> mass-spectrum was made.<sup>20</sup>

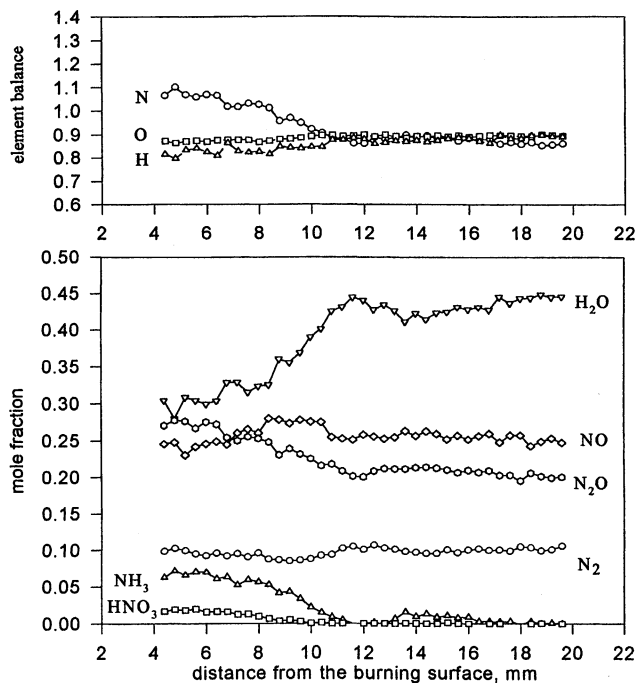
Because many other NO species (N<sub>2</sub>O, NO<sub>2</sub>, HNO<sub>3</sub>, HONO, and ADN<sub>v</sub>) bear an input into peak 30, an error in defining NO by the withdrawn sample mass-spectrum can be large in view of the analysis of NO transformations in chemical reaction zones on ADN burning at 3 atm.

That is why the experiments on the direct quantitative determination of N<sub>2</sub>O to NO concentration ratios in combustion products at 3 atm were carried out. ADN combustion products at 3 atm were passed through a fine purification filter to eliminate AN particles generated on HNO<sub>3</sub> and NH<sub>3</sub> condensation. Peaks with 17, 46, and 63 amu were absent in the product mass-spectra.  $\alpha_{\text{NO}}/\alpha_{\text{N}_2\text{O}} = 0.6$  was used to correct the data resulting from the ADN combustion product mass-spectra analysis. The analysis provided product compositions near the burning surface and in the combustion products set forth in Table 6.

The resulting gas composition provides a satisfactory material ( $\sim 5\%$ ) and energetic balance in the near zone, assuming ADN<sub>v</sub> is present in the gas phase by 3%.

Therefore, the analysis of mass-spectrum of samples taken from the zone near the ADN burning surface at 3 atm has shown that there are gaseous ADN in the near-surface zone. The ADN<sub>v</sub> and HD decomposition in the near-surface zone results in a temperature rise of about 150 K.

ADN flame structure at 6 atm: The experiments on MS probing of ADN flames were performed at this pressure only when a strand mounted at a distance of 1 mm from the probe was immovable. The burning surface is moving outward from the probe at an ADN burning rate. Concentration profiles of ADN flame species at a pressure of 6 atm, starting at 4 mm from the burning surface, and element balances are represented in Fig. 11. Ammonia oxidation with HNO<sub>3</sub> and N<sub>2</sub>O is the main reaction to result in heat release in the gas phase. This reaction gives NO, N<sub>2</sub>, and H<sub>2</sub>O as products. Data on the products composition in ADN flame at 6 atm at 4.4 and 19.6 mm from

**Fig. 11** Species mole fraction profiles and element balances in ADN flame at 6 atm ( $u = 20.3$  mm/s).

the burning surface are tabulated in Table 7. NO<sub>2</sub> is absent at 4.4 mm.

An imbalance by elements throughout the burning zone was 10–20%. The data of two experiments on temperature profile measurements (using the method and thermocouples described in the Experimental Techniques section) in the ADN flame at 6 atm are represented in Fig. 12.

We did not succeed in studying the near-surface zone of the ADN flame at 6 atm because of considerable experimental difficulties associated with a large ADN burning rate at this pressure. However, based on the results of studies at 3 atm there appears to be little doubt about its existence at 6 atm. Thus, we can believe that at least two zones are found on ADN burning at 6 atm and more: The first near-surface low-temperature zone of gaseous ADN and dinitraminic acid decomposition, and the second high-temperature zone of ammonia oxidation with nitric acid. Final ADN combustion products (as well as the final combustion temperature) in the second zone do not correspond to thermodynamical equilibrium. Thermodynamic calculations show that there is no nitrogen oxides in the final products and that they have H<sub>2</sub>O, N<sub>2</sub>, and O<sub>2</sub>. The thermodynamically equilibrium temperature is about 2100 K. Thus, at higher pressures there is a higher-temperature third zone of nitrogen oxide reduction.

Our temperature measurements in gas phases on the ADN strand burning at 40 atm (8 mm in diameter, 16 mm in length) support this conclusion. These measurements were performed using WRe (20%)–WRe (5%) thermocouple (50  $\mu$ m in diameter) armoured with Ceramobond 569 shielding (10  $\mu$ m thick). The thermocouple was II-shaped with a shoulder length of 2 mm arranged in parallel to the strand surface. The thermocouple junction was situated within 1.5 mm of the strand



**Table 7** Product composition (in mole fractions) in ADN flame at 6 atm at the different distances  $L$  from the burning surface

$L$ , mm	$\text{NH}_3$	$\text{H}_2\text{O}$	$\text{NO}$	$\text{N}_2\text{O}$	$\text{N}_2$	$\text{HNO}_3$
4.4	0.07	0.31	0.23	0.28	0.10	0.02
19.6	0	0.45	0.25	0.20	0.11	0

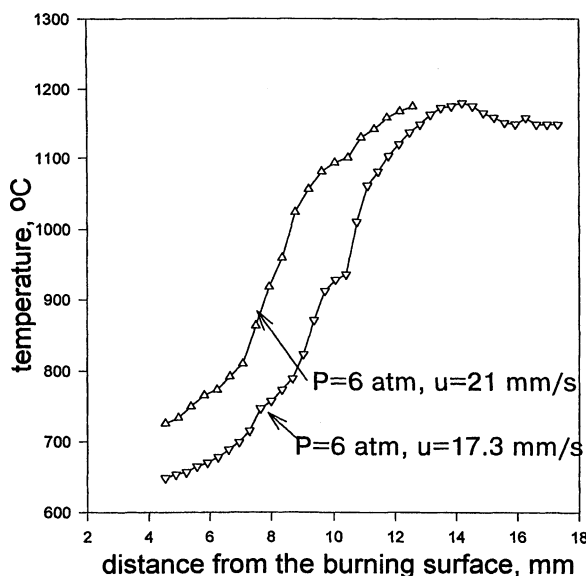


**Fig. 12** Temperature profiles in ADN flame at 6 atm.

surface. The strand burning rate was 50–60 mm/s according to our evaluations. This experiment allows the evaluation of a flame's maximal temperature, which is 2000 K (with a radiation correction).

### Summary and Conclusions

Two MS methods for the study of SP's combustion chemistry in two burning zones, in a condensed phase and in a flame developed by the authors, were further elaborated. To study SP decomposition, reaction kinetics, and mechanisms under conditions closest to those of the burning surface, two variants of MS procedures were developed.

1) For the experiments at pressures of about 1 atm ÷ 6 torr, the study was conducted in a flow reactor connected with an ion source of TOF or quadrupole MS via a molecular beam sampling system.

2) For the experiments at very low pressures of  $\sim 10^{-5}$  torr (which are required to determine decomposition primary products and primary stages), the SP sample was placed near the MS ion source. In both cases the SP sample was placed on a metal ribbon and heated at a high rate (20–200 deg/s) with electric current. The reaction time is about 1 s. To provide a more profound study of ADN sublimation at 6 torr a so-called two-temperature flow reactor was used.

The application of a MBMS setup for the SP thermal decomposition study allowed the detection of an unstable species, which is impossible when using MS with a conventional inlet system. To study the reaction mechanism in an SP flame a method of SP flames probing by MBMS was used. This method provides identification of not only stable species in SP flames but of unstable ones as well, and measurements of their concentrations and their distribution in flames. The field of method application was expanded to 10 atm, which allowed the SP combustion study with conditions close to the ones in the engine chamber. The developed methods were applied to the study of the combustion chemistry of ADN, a new SP oxidizer.

ADN thermal decomposition was studied with TOF and a quadrupole MS at pressures of about  $10^{-6}$ , 6, and 100 torr, and 1 atm within the temperature range of  $\sim 80$ – $300^\circ\text{C}$  at isothermal and nonisothermal conditions. The first-order reaction of decomposition in vacuum has been determined. The reaction rate constant in vacuum was found to be  $W = d\alpha/dt = 3.5 \times 10^{15} [\exp(-32,000/RT)](1-\alpha)$ ,  $\text{s}^{-1}$ . The mass spectra of the decomposition products were recorded. The analysis of the data obtained showed mass-spectra of ADN decomposition products at 1 atm, and 100 and 6 torr to differ significantly from the mass-spectra of ADN decomposition products in vacuum, particularly the ratio  $I_{46}/I_{17}$ , which comprises 1.5–1.7 in the first case, and in vacuum  $I_{46}/I_{17} = 0.06$ – $0.16$ . ADN decomposition at  $80$ – $140^\circ\text{C}$  at 6 torr in the flow reactor showed that more than 90% ADN sublimated. Using a two-temperature reactor it has been shown that ADN at  $140^\circ\text{C}$  sublimates unlike other ammonium salts with the formation of gaseous ADN. The latter decomposes into dinitraminic acid and ammonia at  $160$ – $400^\circ\text{C}$ . Therefore, the existence of gaseous ADN and HD at ADN decomposition has been proved. Gaseous ADN and HD are adsorbed by the vacuum chamber walls when ADN decomposed in vacuum, and that is why they are not found in a mass-spectra.

ADN flame structure was studied at 1 ÷ 6 atm using a MSMS combined with a microthermocouple technique. The flame structure was found to involve three zones. At 1 ÷ 3 atm a luminous flame zone was not observed. The burning rate at 1 ÷ 6 atm was controlled by the reactions in the condensed phase. At 3 atm the "cool" flame zone adjacent to the burning surface was found. The width of this zone is about 1 ÷ 1.5 mm. The following mass peaks were found in mass-spectra of samples taken from the area adjacent to the burning surface at 3 atm (ions responsible for these peaks are cited in parentheses): 63 ( $\text{HNO}_3^+$ ); 62 ( $\text{NH}_2\text{NO}_2^+$ ); 47 ( $\text{HNO}_2^+$ ); 46 ( $\text{NO}_2^+$ ); 45 ( $\text{HN}_2\text{O}^+$ ); 44 ( $\text{N}_2\text{O}^+$ ); 30 ( $\text{NO}^+$ ); 29 ( $\text{N}_2\text{H}^+$ ); 28 ( $\text{N}_2^+$ ); 18 ( $\text{H}_2\text{O}^+$ ); and 17 ( $\text{NH}_3^+$ ,  $\text{OH}^+$ ). The ratio between mass peak intensities in the mass-spectra of samples taken from the zone adjacent to the ADN burning surface at 3 atm and those of the ADN decomposition products are in reasonable agreement. The analysis of mass-spectra of samples taken from the zone near the ADN burning surface at 3 atm showed that gaseous ADN are the key reactants in the near-surface zone. The product compositions near the ADN burning surface were determined. Gaseous ADN decomposition in the near-surface zone resulted in a temperature rise of about 150 K. The second high-temperature zone was found within 6 ÷ 8 mm from the ADN burning surface at 6 atm. The main reaction in this zone is ammonia oxidation by nitric acid. The combustion temperature in this zone is 1400 K and the combustion products are  $\text{H}_2\text{O}$ ,  $\text{NO}$ ,  $\text{N}_2\text{O}$ , and  $\text{N}_2$ . The third zone was observed at 40 atm. The measured final temperature of 2000 K is close to the thermodynamically calculated one (2100 K). The obtained data form the development basis of a chemical mechanism of reactions in both an ADN flame and combustion model.

### Acknowledgment

This work was supported by the U.S. Army Missile Command under Contract DAAH0195CR141, and European Office of Aerospace Research and Development under Contract F61708-97-WO195.

### References

- Edwards, T., "Solid Propellant Flame Spectroscopy," Air Force Lab., TR-88-076, Edwards AFB, CA, 1988.
- Korobeinichev, O. P., "Dynamic Probe Mass Spectrometry of Flames and the Decomposition of Condensed Systems," *Combustion, Explosion and Shock Waves*, Vol. 23, No. 5, 1988, pp. 565–576.
- Korobeinichev, O. P., "A Study of Condensed System Flame Structure," *Pure and Applied Chemistry*, Vol. 65, No. 2, 1993, pp. 269–276.
- Korobeinichev, O. P., Kuibida, L. V., Paletsky, A. A., and Chernov, A. A., "Study of Solid Propellant Flame Structure By Mass-Spectro-

metric Sampling," *Combustion Science and Technology*, Vol. 113, 114, 1996, pp. 557–571.

<sup>5</sup>Litzinger, T. A., Lee, Y. J., and Tang, C. J., "A Study of Solid Propellant Combustion Using a Triple Quadrupole Mass Spectrometer with Microprobe Sampling," *Proceedings of the Workshop on the Application of Free-Jet, Molecular Beam, Mass Spectrometric Sampling* (Estes Park, CO), National Technical Information Service (NTIS), U.S. Dept. of Commerce, Springfield, VA, 1994, pp. 128–135.

<sup>6</sup>Fetherolf, B. L., and Litzinger, T. A., "Physical and Chemical Processes Governing the CO<sub>2</sub> Laser-Induced Deflagration of Ammonium Dinitramide (ADN)," *Proceedings of the 29th JANNAF Combustion Subcommittee Meeting*, Vol. II, 1992, pp. 327–338.

<sup>7</sup>Vanderhoff, J. A., Teague, M. W., and Kotlar, A. J., "Absorption Spectroscopy Through the Dark Zone of Solid Propellant Flame," Ballistic Research Lab. Rept. BRL-TR-3334, 1992.

<sup>8</sup>Parr, T., and Hanson-Parr, D., "Solid Propellant Flame Structure," *Non-Intrusive Combustion Diagnostics*, edited by K. Kuo and T. P. Parr, Begell House Publishing, Inc., New York, 1994, pp. 517–599.

<sup>9</sup>Stufflebeam, J. H., and Eckbreth, A. C., "CARS Diagnostics of Solid Propellant Combustion at Elevated Pressure," *Combustion Science and Technology*, Vol. 66, 1989, pp. 163–179.

<sup>10</sup>Zenin, A. A., "The Temperature Distribution Structure in the Steady Burning of Double-Base Propellants," *Fizika Goreniya i Vzryva*, Vol. 2, No. 3, 1966, pp. 67–76 (in Russian).

<sup>11</sup>Korobeinichev, O. P., and Tereshchenko, A. G., "Mass-Spectrometric Study of Distribution of Concentrations in Combustion Zones of Condensed Systems," *Doklady Akademii Nauk USSR*, Vol. 231, No. 5, 1976, pp. 1159–1161 (in Russian).

<sup>12</sup>Brill, T. B., Brush, P. J., and Patil, D. G., "Thermal Decomposition of Energetics Materials 58. Chemistry of Ammonium Nitrate and Ammonium Dinitramide Near the Burning Surface Temperature," *Combustion and Flame*, Vol. 92, No. 1, 2, 1993, pp. 178–186.

<sup>13</sup>Korobeinichev, O. P., and Anisiforov, G. I., "Mass-Spectrometric Thermal Analysis Using the Time-of-Flight Mass Spectrometer," *Izvestiya Sibirskogo Otdeleniya Akademii Nauk USSR, Seriya Khimicheskaya*, Vol. 4, No. 4, 1974, pp. 38–41 (in Russian).

<sup>14</sup>Pak, Z., "Some Ways to Higher Environmental Safety of Solid Rockets Propellant Application," AIAA Paper 93-1755, 1993.

<sup>15</sup>Mebel, A. M., Lin, M. C., Morokuma, K., and Melius, C. F., "Theoretical Study of the Gas-Phase Structure, Thermochemistry and Decomposition Mechanisms of NH<sub>4</sub>NO<sub>2</sub> and NH<sub>4</sub>N(NO<sub>2</sub>)<sub>2</sub>," *Journal of Physical Chemistry*, Vol. 99, No. 18, 1995, pp. 6842–6848.

<sup>16</sup>Manelis, G. B., "Kinetics and Mechanism of ADN Thermal Decomposition Pyrotechnics, Basic Principles, Technology, Application," *26th Annual Conference of ICT*, DWS Werbeagentur und Verlag GmbH, Karlsruhe, Germany, Vol. 15, 1995, pp. 1–17.

<sup>17</sup>Fogelzang, A. E., Sinditskii, V. P., Egorshv, V. Y., Levshenkov, A. I., Serushkin, V. V., and Kolesov, V. I., "Combustion Behavior and Flame Structure of Ammonium Dinitramide," *Combustion and Detonation, 28th Annual Conference of ICT*, Vol. 99, DWS Werbeagentur und Verlag GmbH, Karlsruhe, Germany, 1997, pp. 1–14.

<sup>18</sup>Korobeinichev, O. P., Kuibida, L. V., Paletsky, A. A., and Shmakov, A. G., "Study of Flame Structure, Kinetics and Mechanism of the Thermal Decomposition of Solid Propellants by Probing Mass-Spectrometry," *Challenges in Propellant and Combustion 100 Years After Nobel*, edited by Kenneth K. Kuo, Begell House Inc., New York, 1997, pp. 38–47.

<sup>19</sup>Korobeinichev, O. P., Kuibida, L. V., Paletsky, A. A., and Shmakov, A. G., "Combustion Chemistry of Energetic Materials Studied by Probing Mass-Spectrometry," *Proceedings of the Material Research Society Symposium*, Vol. 418, Material Research Society, Pittsburgh, PA, 1996, pp. 245–255.

<sup>20</sup>Rossi, M. J., Bottaro, J. C., and McMillen, D. F., "The Thermal Decomposition of the New Energetic Material Ammonium Dinitramide (NH<sub>4</sub>N(NO<sub>2</sub>)<sub>2</sub>) in Relation to Nitramide (NH<sub>2</sub>NO<sub>2</sub>) and NH<sub>4</sub>NO<sub>3</sub>," *International Journal of Chemical Kinetics*, Vol. 25, 1993, pp. 549–570.

<sup>21</sup>Vyazovkin, S., and Wight, C. A., "Ammonium Dinitramide: Kinetics and Mechanism of Thermal Decomposition," *Journal of Physical Chemistry A*, Vol. 101, No. 31, 1997, pp. 5653–5658.

<sup>22</sup>Vyazovkin, S., and Wight, C. A., "Thermal Decomposition of Ammonium Dinitramide at Moderate and High Temperatures," *Journal of Physical Chemistry*, Vol. 101, 1997, pp. 7217–7221.

<sup>23</sup>Oxley, J. C., Smith, J. L., Zheng, W., Rogers, E., and Coburn, M. D., "Thermal Decomposition Studies on Ammonium Dinitramide (ADN) and <sup>15</sup>N & <sup>2</sup>H Isotopomers," *Journal of Physical Chemistry*, Vol. 101, 1997.

<sup>24</sup>Russell, T. P., Stern, A. G., Koppes, W. M., and Bedford, D. C., "Thermal Decomposition and Stabilization of Ammonium Dinitramide," *Proceedings of the JANNAF Combustion Meeting*, Vol. II, Chemical Propulsion Information Agency, Hampton, VA, 1992, p. 339.

<sup>25</sup>Politzer, P., Seminario, J. M., and Concha, M. C., "Energetics of Ammonium Dinitramide Decomposition Steps," *Journal of Molecular Structure (Theochem)*, (to be published).

<sup>26</sup>Lobbecke, S., Krause, H. H., and Pfeil, A., "Thermal Analysis of Ammonium Dinitramide Decomposition," *Propellants, Explosives, Pyrotechnics*, Vol. 22, 1997, pp. 184–188.

<sup>27</sup>Parr, T., and Hanson-Parr, D. M., "Solid Propellant Diffusion Flame Structure," 26th Symposium (International) on Combustion, The Combustion Institute, Pittsburgh, PA, 1996.

<sup>28</sup>Korobeinichev, O. P., Paletsky, A. A., Kuibida, L. V., Bolshova, T. A., and Fristrom, R. M., "Study of the Structure of a Ten Atmosphere H<sub>2</sub>/O<sub>2</sub>/Ar Flame Using Molecular Beam Inlet Mass Spectrometric Probing," *Fizika Goreniya i Vzryva*, Vol. 32, No. 3, 1996, pp. 3–10 (in Russian).

<sup>29</sup>Korobeinichev, O. P., Boldyrev, V. V., Karpenko, Yu. Y., "Use of an Impulse Mass-Spectrometer to Study the Kinetics of Fast Processes During High-Temperature Decomposition of Ammonium Perchlorate," *Fizika Goreniya i Vzryva*, Vol. 4, No. 1, 1968, pp. 33–38 (in Russian).

<sup>30</sup>Korobeinichev, O. P., "Use of Mass-Spectrometry to Study the Kinetics and Mechanism of the Decomposition in Solids," *Uspehi Khimii*, Vol. 38, No. 12, 1969, pp. 2113–2128 (in Russian).

<sup>31</sup>Korobeinichev, O. P., Anisiforov, G. I., and Tereshchenko, A. G., "High-Temperature Decomposition of Ammonium Perchlorate-Polystyrene-Catalyst Mixtures," *AIAA Journal*, Vol. 13, No. 5, 1975, pp. 628–633.

<sup>32</sup>Korobeinichev, O. P., Ilyin, S. B., Mokrushin, V. V., and Shmakov, A. G., "Destruction Chemistry of Dimethyl Methylphosphonate in H<sub>2</sub>/O<sub>2</sub>/Ar Flame Studied by Molecular Beam Mass Spectrometry," *Combustion Science and Technology*, Vol. 116, 1996, pp. 51–67.

<sup>33</sup>Luk'yanov, A. O., Gorelik, V. D., and Tartakovsky, V. A., "Ammonium Dinitramide and Its Salts," *Izvestiya Akademii Nauk, Seriya Khimicheskaya*, Vol. 1, 1994, pp. 94–97 (in Russian).